Superconductivity in doped Sr_2IrO_4: A functional renormalization group study

Yang Yang,[1] Wan-Sheng Wang,[1] Jin-Guo Liu,[1] Hua Chen,[2] Jian-Hui Dai,[3] and Qiang-Hua Wang[1]
[1]*National Laboratory of Solid State Microstructures & School of Physics, Nanjing University, Nanjing 210093, China*
[2]*Zhejiang Institute of Modern Physics & Department of Physics, Zhejiang University, Hangzhou 310027, China*
[3]*Department of Physics, Hangzhou Normal University, Hangzhou 310036, China*
(Received 18 December 2013; revised manuscript received 10 March 2014; published 25 March 2014)

Using the functional renormalization group we investigated possible superconductivity in doped Sr_2IrO_4. In the electron-doped case, a $d^*_{x^2-y^2}$-wave superconducting phase is found in a narrow doping region. The pairing is driven by spin fluctuations within the single conduction band. In contrast, for hole doping an $s^*_\pm$-wave phase is established, triggered by spin fluctuations within and across the two conduction bands. In all cases there are comparable singlet and triplet components in the pairing function. The Hund's rule coupling reduces (enhances) superconductivity for electron (hole) doping. Our results imply that hole doping is more promising to achieve a higher transition temperature. Experimental perspectives are discussed.

DOI: 10.1103/PhysRevB.89.094518 PACS number(s): 71.27.+a, 74.20.Rp

I. INTRODUCTION

Recently, the iridium oxide Sr_2IrO_4 has been subject to extensive investigations [1–11]. In the parent compound the Ir atom is in the $5d^5$ configuration. The spin-orbital coupling (SOC) splits the t_{2g} manifold into filled $J = 3/2$ multiplets and half-filled $J = 1/2$ doublets, leading to the band structure shown in Fig. 1. Since the top $J = 1/2$ band is half filled and the width is narrowed down to the scale of local interactions, the parent compound was argued to be a Mott insulator. Indeed, transport measurements revealed insulating behavior [3], and a canted antiferromagnetic (AFM) order was found in x-ray scattering and neutron diffraction measurements [7–11]. In analogy to cuprates, an intriguing issue is whether superconductivity (SC) could be realized by doping the parent insulator [9,12].

Theoretically, a variational Monte Carlo (VMC) study of Sr_2IrO_4 [13] suggests that d-wave SC may appear but only within a narrow region of electron doping. The absence of SC in the hole-doped side is not straightforward to understand. In fact, by sufficient hole doping, both of the two higher bands are cut by the Fermi level (see Fig. 1), forming Fermi pockets around the Γ and M points in the Brillouin zone. (In this case the band structure raises questions about the notion of Sr_2IrO_4 as a doped Mott insulator.) Instead, the Fermi surface topology is closely similar to that in iron pnictides, where interpocket scattering proves to be very efficient in driving $s_\pm$-wave superconductivity [14,15]. However, this does not seem to be the case in the VMC results. Given the unavoidable bias in VMC calculations, we think it beneficial to perform a complementary, yet unbiased, search for SC in doped Sr_2IrO_4.

In this paper we resort to the functional renormalization group (FRG) [16]. This is because the FRG treats all electronic instabilities on equal footing without *a priori* assumption about the candidate order parameters. It has proved successful in doped cuprates and iron pnictides [17,18]. We limit ourselves to sufficient electron or hole doping so that the FRG has a better chance of being reliable, as in practice for doped cuprates [19]. Since the three bands overlap within an energy window of order 1 eV, as seen in Fig. 1, we include all of the t_{2g} orbitals, and apply the recently developed singular-mode functional renormalization group (SMFRG) [21–28]. Compared to the other FRG schemes, it has the additional advantage of dealing with orbital and spin degrees of freedom and the SOC among them in a more straightforward manner.

Our main findings are as follows: In the electron-doped case, a $d^*_{x^2-y^2}$-wave superconducting phase is found in a narrow doping region close to the Van Hove singularity, in agreement with VMC results. The pairing is driven by spinlike fluctuations within the single conduction band. In contrast, for hole doping an $s^*_\pm$-wave phase is established, triggered by spin fluctuations within and across the two conduction bands. In all cases there are comparable singlet and triplet components in the pairing function. The Hund's rule coupling reduces (enhances) superconductivity in the electron- (hole-) doped case. In view of the reasonable Hund's rule coupling, the doping range, and the pairing scale, we propose that hole doping is more promising for achieving a higher transition temperature. Experimental perspectives are discussed.

II. MODEL AND METHOD

We begin with specification of the model Hamiltonian H. The free part H_0 of H contains the spin-invariant kinetic part $H_{\rm kin}$, and an atomic SOC part $H_{\rm SOC} = -\frac{1}{2}\lambda\sum_j \psi_j^\dagger \mathbf{L}\cdot\boldsymbol{\sigma}\psi_j$, where ψ_j is the annihilation field operator at site j, and $\mathbf{L}$ and $\sigma/2$ are the operators for the orbital and spin angular momenta. To be specific, the nonzero elements of $\mathbf{L} = (L_x, L_y, L_z)$ in the orbital basis (d_{xz}, d_{yz}, d_{xy}) are

$$L_x^{31} = -L_x^{13} = L_y^{23} = -L_y^{32} = L_z^{12} = -L_z^{21} = i. \quad (1)$$

We take $H_{\rm kin}$ suggested in Refs. [13,20], where the effect of lattice distortions [2,12] has been taken into account. For SOC we set $\lambda = 0.5$ eV. The corresponding band structure and density of states (DOS) for $H_0 = H_{\rm kin} + H_{\rm SOC}$ are shown in Figs. 1(a) and 1(b), respectively. (Notice that each band remains twofold degenerate.) The horizontal line B corresponds to the undoped Fermi level and the other lines to the doped cases to be addressed specifically later.

The interacting part H_I of H contains intraorbital repulsion U, interorbital repulsion U', Hund's rule spin exchange J, and pair hopping J'. The explicit form of H_I is standard and can be found elsewhere [26]. We apply the Kanamori relations $U = U' + 2J$ and $J = J'$ to reduce the number of independent parameters. According to an estimate by the constrained

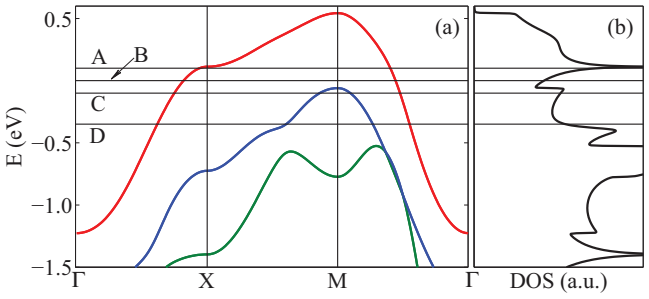

FIG. 1. (Color online) (a) The electronic structure of Sr_2IrO_4 described by $H_0 = H_{\rm kin} + H_{\rm SOC}$, with $H_{\rm kin}$ from Refs. [13,20]. Each band remains doubly degenerate. The horizontal lines indicate Fermi levels addressed in the text. The Fermi energy of the undoped compound is set to zero (line B). (b) Normal-state density of states.

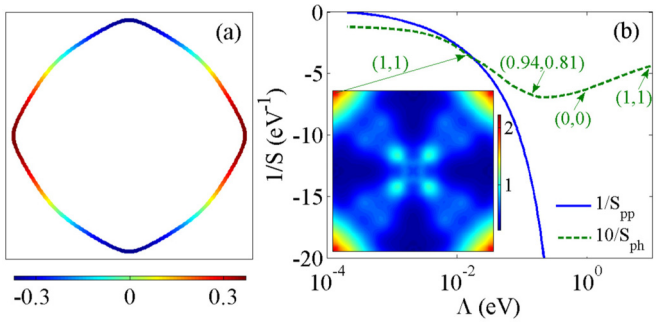

FIG. 2. (Color online) Results for $n = 5.20$. (a) Fermi surface and gap function $\Delta(\mathbf{k})$ (color scale). (b) FRG flow of $1/S_{ph,pp}$, the inverse of the leading attractive interactions, versus the running energy scale Λ. Notice that $1/S_{pp,ph} \to 0^-$ if $S_{pp,ph}$ diverges. The arrows indicate snapshots of the leading momentum $\mathbf{Q}$ (divided by π) in the p-h channel. The inset shows $\ln|S_{ph}(\mathbf{q})|$ in the Brillouin zone at the final energy scale.

random phase approximation [29], we limit ourselves to the parameter ranges $U = 2$–3 eV and $J/U = 0.05$–0.20.

The bare interactions, upon full antisymmetrization, provide the initial values of the running interaction vertices (versus a decreasing energy scale) in the SMFRG. A general interaction vertex function can be decomposed as

$$V^{\alpha,\beta;\gamma,\delta}_{\mathbf{k},\mathbf{k}',\mathbf{q}} \to \sum_m S_m(\mathbf{q})\phi^{\alpha,\beta}_m(\mathbf{k},\mathbf{q})\big[\phi^{\gamma,\delta}_m(\mathbf{k}',\mathbf{q})\big]^*, \qquad (2)$$

either in the particle-particle (p-p) or particle-hole (p-h) channel. Here, $(\alpha,\beta,\gamma,\delta)$ are dummy labels for orbital and spin indices, $\mathbf{q}$ is the collective momentum, and $\mathbf{k}$ (or $\mathbf{k}'$) is the internal momentum of the fermion bilinears $\psi^\dagger_{\mathbf{k}+\mathbf{q},\alpha}\psi^\dagger_{-\mathbf{k},\beta}$ and $\psi^\dagger_{\mathbf{k}+\mathbf{q},\alpha}\psi_{\mathbf{k},\beta}$ in the p-p and p-h channels, respectively. The fastest-growing eigenvalue $S(\mathbf{Q})$ implies an emerging order associated with a collective wave vector $\mathbf{Q}$ and eigenfunction (or form factor) $\phi(\mathbf{k},\mathbf{Q})$ [30]. In the p-p channel $\mathbf{Q} = \mathbf{0}$ is always realized at a low energy scale due to the Cooper mechanism. More technical details can be found elsewhere [21,22].

III. ELECTRON DOPING

We first discuss the electron-doped case with the band filling $n = 5.20$, corresponding to line A in Fig. 1. The Fermi surface is contributed by the upper band alone, as shown in Fig. 2(a), but we should emphasize that our SMFRG includes virtual excitations from all bands. Fig. 2(b) shows the FRG flow of the leading eigenvalues $S_{pp,ph}$ versus the running energy scale Λ (the infrared cutoff of the Matsubara frequency) for $U = 2.4$ eV and $J/U = 0.055$. Apart from some intermediate deviations the momentum associated with S_{ph} is close to $\mathbf{Q} = (\pi,\pi)$. The inset shows $S_{ph}(\mathbf{q})$ versus $\mathbf{q}$ at the final energy scale. There is a broad peak around $\mathbf{Q}$. We checked that the associated form factors describe site-local spins aligned in the plane. Thus AFM spin fluctuations with *easy-plane anisotropy* exist. The enhancement of such spin fluctuations can be ascribed to the quasinesting of the Fermi surface shown in Fig. 2(a) and the proximity to the Van Hove singularity near X (see Fig. 1). The easy-plane anisotropy is from SOC, and appears to be consistent with the easy-plane AFM order in the parent compound [7–11], although the FRG cannot access the Mott limit.

From Fig. 2(b), we see that, as S_{ph} is enhanced below $\Lambda = 0.1$ eV, it triggers S_{pp} to increase and eventually diverge. Therefore the driving force of pairing here is the AFM spin fluctuation discussed above. We write the (matrix) pairing form factor as

$$\phi_{pp}(\mathbf{k}) = (g_{\mathbf{k}} + \gamma_{\mathbf{k}})\, i\sigma_2, \qquad (3)$$

with singlet and triplet parts $g_{\mathbf{k}}$ and $\gamma_{\mathbf{k}}$, respectively. To describe the momentum dependence, we introduce the lattice harmonics

$$c_x = \cos k_x, \quad c_y = \cos k_y. \qquad (4)$$

The nonvanishing elements of $g_{\mathbf{k}}$ and $\gamma_{\mathbf{k}}$ in the orbital basis are

$$\begin{aligned} g^{11/22}_{\mathbf{k}} &\sim (\mp 0.35 \pm 0.20 c_{y/x} \mp 0.08 c_{x/y})\,\sigma_0, \\ g^{33}_{\mathbf{k}} &\sim 0.07(c_y - c_x)\sigma_0, \end{aligned} \qquad (5)$$

$$\begin{aligned} \gamma_{\mathbf{k}} \sim\ & (0.12c_x - 0.15c_y)L_x\sigma_1 + (0.15c_x - 0.12c_y)L_y\sigma_2 \\ & + 0.23(c_x - c_y)L_z\sigma_3. \end{aligned} \qquad (6)$$

Combining the transformation property of the d orbitals [31], we see that $g_{\mathbf{k}}$ transforms as $d_{x^2-y^2}$. The symmetry is consistent with the fact that spin fluctuations at the wave vector $\mathbf{Q} = (\pi,\pi)$ overlap with the $d_{x^2-y^2}$-wave singlet pairing interaction in square lattices. The triplet parts mainly arise from nearest-neighbor bonds and are orbital singlets (i.e., odd in orbital space). We notice that $\gamma_{\mathbf{k}}$ is comparable to $g_{\mathbf{k}}$ and is a result of significant SOC. Under point group operations of spin, orbital, and momentum, $\gamma_{\mathbf{k}}$ also transforms as $d_{x^2-y^2}$. According to Ref. [26] we dub the symmetry of the total pairing function as $d^*_{x^2-y^2}$. The pairing function respects time-reversal symmetry, which could have been anticipated since the d-wave representations on square lattices are nondegenerate. We project the pairing function in the band basis as

$$\Delta_{\mathbf{k}} = \langle\mathbf{k}|\phi_{pp}(\mathbf{k})(|-\mathbf{k}\rangle)^* = \langle\mathbf{k}|g_{\mathbf{k}} + \gamma_{\mathbf{k}}|\mathbf{k}\rangle, \qquad (7)$$

where $|\mathbf{k}\rangle$ is a Bloch state and $|-\mathbf{k}\rangle = i\sigma_2 K|\mathbf{k}\rangle$ is the time reversal of $|\mathbf{k}\rangle$. The gap function $\Delta_{\mathbf{k}}$ is shown in Fig. 2(a)

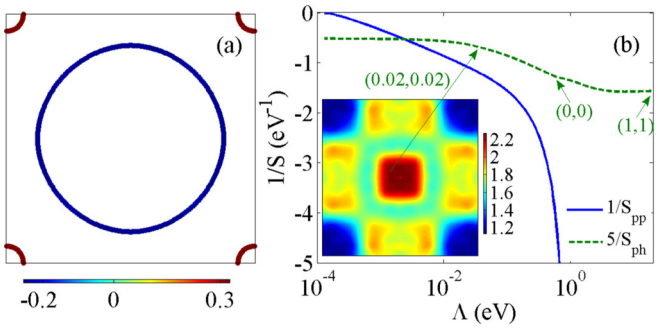

FIG. 3. (Color online) As Fig. 2, except that $n = 4.83$.

(color scale) on one of the doubly degenerate Fermi surfaces, revealing the d-wave sign structure consistent with the above symmetry analysis in the spin-orbital basis. We notice that the gap function does not change between the degenerate Fermi surfaces. This is because any band dependence is determined by $\langle \mathbf{k}|\gamma_{\mathbf{k}}|\mathbf{k}\rangle$, but $\gamma_{\mathbf{k}}$ is of the same form as the SOC, which nonetheless does not break the degeneracy. We notice in passing that the pairing function in the orbital basis in this paper would be useful in further VMC studies.

IV. HOLE DOPING

We now discuss the hole-doped cases. First consider a band filling $n = 4.83$ associated with line C in Fig. 1. The Fermi surface topology changes drastically. A large Γ pocket from the upper band and a small M pocket from the middle band appear, as shown in Fig. 3(a). For reasons to be clearer later, we set $U = 2.4$ eV and $J/U = 0.175$, with a larger Hund's rule coupling. The FRG flow is shown in Fig. 3(b). In this case, the $\mathbf{Q}$ vector for the leading S_{ph} evolves from (π,π) at high energy scales to small momenta at moderate and low energy scales. The inset shows $S_{ph}(\mathbf{q})$ versus $\mathbf{q}$ at the final energy scale. Incommensurate peaks around the zone center are obvious. The fact that they are stronger at low energy scales suggests that they arise from intrapocket scattering around M. We checked that such fluctuations are also spinlike, but now the fluctuating spins are aligned along the out-of-plane directions. Thus hole doping leads to ferromagneticlike spin fluctuations with easy-axis anisotropy. The difference from the electron-doped case can be easily checked, e.g., by neutron scattering. On the other hand, there are secondary peaks at $\mathbf{Q}' \sim (\pi,\pi/4)$ and its symmetry images in $S_{ph}(\mathbf{q})$. They are also spinlike as shown by checking the associated form factors. These spin fluctuations can come only from interpocket (thus interband in our case) scattering. From Fig. 3(b), as spin fluctuations are enhanced in the intermediate energy window, the attractive pairing interaction S_{pp} is induced rapidly and eventually diverges. At this stage, we find the following nonvanishing elements for $\phi_{pp}(\mathbf{k})$:

$$g_{\mathbf{k}}^{11/22} \sim (0.15c_{x/y} + 0.02c_{y/x})\sigma_0,$$
$$g_{\mathbf{k}}^{33} \sim [0.37 - 0.03(c_x + c_y)]\sigma_0, \tag{8}$$

$$\gamma_{\mathbf{k}} \sim 0.07(L_x\sigma_1 + L_y\sigma_2) + [0.40 - 0.05(c_x + c_y)]L_z\sigma_3. \tag{9}$$

Symmetry analysis similar to that in the previous case shows that the gap function transforms as s wave [31]. The singlet and triplet parts are comparable in magnitude and both are time-reversal invariant. The projection of $\phi_{pp}(\mathbf{k})$, or $\Delta(\mathbf{k})$, is shown in Fig. 3(a) (color scale). We see that $\Delta(\mathbf{k})$ is roughly isotropic on each pocket, but changes sign from the Γ to the M pocket. Combined with the admixture of singlets and triplets in the orbital basis, we dub the global pairing symmetry as $s_{\pm}^*$ wave [32]. For the singlet part the sign change across the pockets takes advantage of the scattering provided by the secondary spin fluctuations near $\mathbf{Q}'$ mentioned above. We conclude that pairing is driven by spin fluctuations within the holelike band, and further enhanced by the interpocket scattering in the two conduction bands. The reason that the interpocket scattering is not leading is because the electron and hole pockets are poorly nested.

We find that the above picture also applies for higher levels of hole doping, except that the wave vector $\mathbf{Q}$ of the leading spin fluctuations becomes larger (since the hole pocket is enlarged) and $\mathbf{Q}'$ for the subleading ones becomes closer to (π,π) (since the quasinesting between the pockets is improved). Instead of repeating the discussions, we provide the pairing function for $n = 4.25$ (in view of its potential application in VMC simulations), associated with line D in Fig. 1,

$$g_{\mathbf{k}}^{11/22} \sim [-0.11 - 0.30(c_x + c_y)]\sigma_0,$$
$$g_{\mathbf{k}}^{33} \sim [-0.21 - 0.14(c_x + c_y)]\sigma_0, \tag{10}$$

$$\gamma_{\mathbf{k}} \sim (0.17 - 0.02c_x - 0.12c_y)L_x\sigma_1 + (0.17 - 0.12c_x - 0.02c_y)L_y\sigma_2 + [0.19 + 0.04(c_x + c_y)]L_z\sigma_3, \tag{11}$$

obtained with the same parameters U and J as above. The pairing symmetry remains $s_{\pm}^*$ wave. We notice that at this level of hole doping, the hole pocket is quasinested, and this leads to stronger intrapocket spin fluctuations and hence stronger SC (see below).

V. SYSTEMATICS

We have performed systematic calculations by varying the bare interaction parameters. Figure 4 shows the critical scale

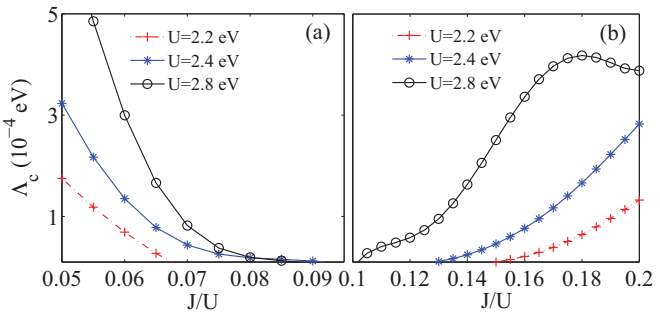

FIG. 4. (Color online) The superconducting critical scale Λ_c versus J/U for various U. (a) The $d^*_{x^2-y^2}$-wave pairing at electron doping $n = 5.20$. (b) The $s_{\pm}^*$-wave pairing at hole doping $n = 4.83$.

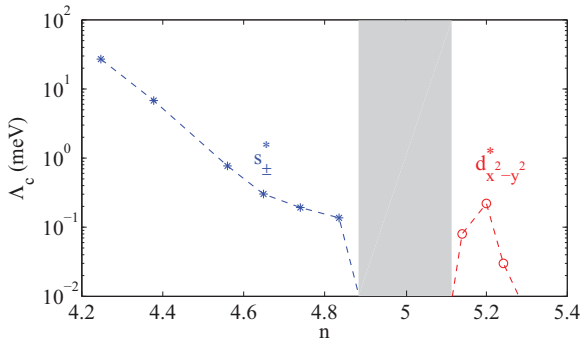

FIG. 5. (Color online) The superconducting critical scale Λ_c versus doping. Here $U = 2.4$ eV and $J/U = 0.055$ (0.175) for electron (hole) doping.

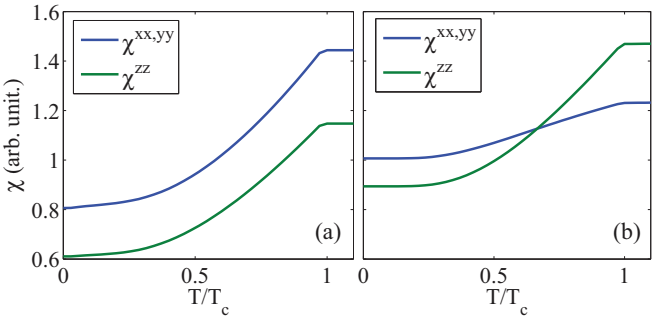

FIG. 6. (Color online) Spin susceptibilities $\chi^{xx,yy,zz}$ as functions of temperature for (a) $d^*_{x^2-y^2}$-wave pairing in the electron-doped case $n = 5.20$ and (b) $s^*_\pm$-wave pairing in the hole-doped case $n = 4.83$. Here T_c is the mean-field transition temperature.

Λ_c, the energy scale at which the superconducting instability occurs, versus J/U for various values of U. For a fixed J/U, Λ_c increases with U. The effect of J for a fixed U is highly nontrivial, however. In the electron-doped case, Fig. 4(a) shows that the Hund's coupling J suppresses Λ_c for $d^*_{x^2-y^2}$-wave pairing in the electron-doped case. On the contrary, in the hole-doped case $s^*_\pm$-wave pairing is enhanced by J, as shown in Fig. 4(b). The systematics is consistent with the fact that the Hund's rule coupling favors spin fluctuations at smaller wave vectors. Judging from Fig. 4 we conclude that hole doping is more promising for achieving a higher transition temperature for a reasonable Hund's rule coupling (e.g., $J/U \geqslant 0.1$.)

On the other hand, we have also performed systematic calculations by varying the filling level n. Figure 5 shows the n dependence of Λ_c. The grayed region is not considered since it is too close to the Mott insulating limit for FRG to be reliable. We are interested in sufficient electron- or hole-doping away from this region. We set $U = 2.4$ eV here for illustration. In principle we also need to fix J to have a fair comparison between electron and hole doping. However, since J is badly unfavorable in the electron-doped case ($n > 5$), we set $J/U = 0.055$ just in order to have a sizable Λ_c. Even in this case, SC exists only within a narrow doping region around $n = 5.2$ (close to the Van Hove filling), in agreement with the VMC result. Instead, in the hole-doped case ($n < 5$), we set a reasonable value $J/U = 0.175$ for definiteness. We see that the SC phase extends for all $n \leqslant 4.83$, and Λ_c is enhanced up to $\Lambda_c \sim 30$ meV for $n = 4.25$. This pairing scale is of the same order as that in iron pnictides, and we conclude that the deeply hole-doped Sr_2IrO_4 could be a high-T_c superconductor.

VI. EXPERIMENTAL PERSPECTIVES

We discuss some experimental consequences regarding the pairing functions obtained so far. Since the $d^*_{x^2-y^2}$-wave pairing has a nodal gap on the Fermi surface, while the $s^*_\pm$-wave pairing is fully gapped, they can be easily differentiated by low-temperature thermodynamic measurements (such as the specific heat and superfluid density) and by spectroscopic measurements (such as angle-resolved photoemission and scanning tunneling microscopy). The change of spin anisotropy can be easily probed by neutron diffraction. However, since both types of pairing involve comparable mixing of singlets and triplets, the difference in the spin susceptibility is not as straightforward. We performed mean-field calculations in both cases, with the pairing interaction derived from the SMFRG (slightly before the divergence scale), and calculated the direction-resolved spin susceptibilities $\chi^{xx,yy,zz}$ versus temperature T. The results are shown in Fig. 6(a) for $d^*_{x^2-y^2}$- and (b) for $s^*_\pm$-wave pairing for $n = 5.20$ and $n = 4.83$, respectively. In both cases the susceptibilities are above 40% of the normal-state value as $T \to 0$, and there is anisotropy between (χ^{xx}, χ^{yy}) versus χ^{zz}. Such behaviors, combined with the spectroscopic measurements, would provide an unambiguous probe of the pairing functions predicted here.

VII. CONCLUSIONS AND REMARKS

To conclude, in electron- (or hole-) doped Sr_2IrO_4, a $d^*_{x^2-y^2}$-wave (or $s^*_\pm$-wave) superconducting phase is possible. They are triggered by in-plane AFM spin fluctuations for electron doping, and by out-of-plane spin fluctuations within the hole pocket, as well as from interpocket scattering [33]. In all cases there are comparable singlet and triplet components. The effect of Hund's rule coupling J suppresses (enhances) SC in the electron- (hole-) doped region significantly. A reasonable value of $J/U \geqslant 0.1$ makes hole doping more promising for achieving a higher transition temperature. Experimental perspectives are discussed.

We notice that superconductivity has not been observed yet experimentally after electron doping [34]. While further efforts are needed, *our results for hole doping stimulate a different direction*. Experimentally, hole doping can be achieved by substituting K or Na for Sr in Sr_2IrO_4. Presently isovalent substitution of Ca or Ba for Sr [35] and partial substitution of Ru for Ir have been reported [36].

ACKNOWLEDGMENTS

The project was supported by NSFC (under Grants No. 11023002 and No. 11274084) and the Ministry of Science and Technology of China (under Grants No. 2011CBA00108 and No. 2011CB922101).

[1] J. J. Randall, L. Katz, and R. Ward, J. Am. Chem. Soc. **79**, 266 (1957).

[2] M. K. Crawford, M. A. Subramanian, R. L. Harlow, J. A. Fernandez-Baca, Z. R. Wang, and D. C. Johnston, Phys. Rev. B **49**, 9198 (1994).

[3] G. Cao, J. Bolivar, S. McCall, J. E. Crow, and R. P. Guertin, Phys. Rev. B **57**, R11039 (1998).

[4] B. J. Kim, H. Jin, S. J. Moon, J.-Y. Kim, B.-G. Park, C. S. Leem, J. Yu, T. W. Noh, C. Kim, S.-J. Oh, J.-H. Park, V. Durairaj, G. Cao, and E. Rotenberg, Phys. Rev. Lett. **101**, 076402 (2008).

[5] M. F. Cetin, P. Lemmens, V. Gnezdilov, D. Wulferding, D. Menzel, T. Takayama, K. Ohashi, and H. Takagi, Phys. Rev. B **85**, 195148 (2012).

[6] S. J. Moon, H. Jin, W. S. Choi, J. S. Lee, S. S. A. Seo, J. Yu, G. Cao, T. W. Noh, and Y. S. Lee, Phys. Rev. B **80**, 195110 (2009).

[7] B. J. Kim, H. Ohsumi, T. Komesu, S. Sakai, T. Morita, H. Takagi, and T. Arima, Science **323**, 1329 (2009).

[8] K. Ishii, I. Jarrige, M. Yoshida, K. Ikeuchi, J. Mizuki, K. Ohashi, T. Takayama, J. Matsuno, and H. Takagi, Phys. Rev. B **83**, 115121 (2011).

[9] J. Kim, D. Casa, M. H. Upton, T. Gog, Y.-J. Kim, J. F. Mitchell, M. van Veenendaal, M. Daghofer, J. van den Brink, G. Khaliullin, and B. J. Kim, Phys. Rev. Lett. **108**, 177003 (2012).

[10] S. Fujiyama, H. Ohsumi, T. Komesu, J. Matsuno, B. J. Kim, M. Takata, T. Arima, and H. Takagi, Phys. Rev. Lett. **108**, 247212 (2012).

[11] F. Ye, S. Chi, B. C. Chakoumakos, J. A. Fernandez-Baca, T. Qi, and G. Cao, Phys. Rev. B **87**, 140406(R) (2013).

[12] F. Wang and T. Senthil, Phys. Rev. Lett. **106**, 136402 (2011).

[13] H. Watanabe, T. Shirakawa, and S. Yunoki, Phys. Rev. Lett. **110**, 027002 (2013).

[14] Y. Kamihara, T. Watanabe, M. Hirano, and Hideo Hosono, J. Am. Chem. Soc. **130**, 3296 (2008).

[15] I. I. Mazin, D. J. Singh, M. D. Johannes, and M. H. Du, Phys. Rev. Lett. **101**, 057003 (2008).

[16] C. Wetterich, Nucl. Phys. B **352**, 529 (1991).

[17] See. e.g., M. Salmhofer and C. Honerkamp, Prog. Theor. Phys. **105**, 1 (2001); C. Honerkamp, M. Salmhofer, N. Furukawa, and T. M. Rice, Phys. Rev. B **63**, 035109 (2001).

[18] F. Wang, H. Zhai, Y. Ran, A. Vishwanath, and D.-H. Lee, Phys. Rev. Lett. **102**, 047005 (2009).

[19] C. Honerkamp, H. C. Fu, and D. H. Lee, Phys. Rev. B **75**, 014503 (2007).

[20] H. Watanabe, T. Shirakawa, and S. Yunoki, Phys. Rev. Lett. **105**, 216410 (2010).

[21] W.-S. Wang, Y.-Y. Xiang, Q.-H. Wang, F. Wang, F. Yang, and D.-H. Lee, Phys. Rev. B **85**, 035414 (2012).

[22] Y.-Y. Xiang, W.-S. Wang, Q.-H. Wang, and D.-H. Lee, Phys. Rev. B **86**, 024523 (2012).

[23] Y.-Y. Xiang, F. Wang, D. Wang, Q.-H. Wang, and D.-H. Lee, Phys. Rev. B **86**, 134508 (2012).

[24] W.-S. Wang, Z.-Z. Li, Y.-Y. Xiang, and Q.-H. Wang, Phys. Rev. B **87**, 115135 (2013).

[25] Y.-Y. Xiang, Y. Yang, W.-S. Wang, Z.-Z. Li, and Q.-H. Wang, Phys. Rev. B **88**, 104516 (2013).

[26] Y. Yang, W.-S. Wang, Y.-Y. Xiang, Z.-Z. Li, and Q.-H. Wang, Phys. Rev. B **88**, 094519 (2013).

[27] Q. H. Wang, C. Platt, Y. Yang, C. Honerkamp, F. C. Zhang, W. Hanke, T. M. Rice, and R. Thomale, Europhys. Lett. **104**, 17013 (2013).

[28] W.-S. Wang, Y. Yang, and Q. H. Wang, arXiv:1312.3071.

[29] R. Arita, J. Kuneš, A. V. Kozhevnikov, A. G. Eguiluz, and M. Imada, Phys. Rev. Lett. **108**, 086403 (2012).

[30] Notice that all **Q** vectors have symmetry images and could evolve with the running energy scale.

[31] Notice that upon point group operations the orbitals also change. See, e.g., Y. Wan and Q.-H. Wang, Europhys. Lett. **85**, 57007 (2009).

[32] Apart from the important triplet components, the $s^*_{\pm}$ pairing is an interesting analog of the $s_{\pm}$ pairing in iron pnictides.

[33] A. similar change of pairing symmetry was observed in an artificial double-layer Hubbard model where SOC is absent and the pairing is driven by AFM spin fluctuations alone. See, e.g., F. Wang, H. Zhai, and D. H. Lee, Europhys. Lett. **85**, 37005 (2009); W. Cho, R. Thomale, S. Raghu, and S. A. Kivelson, Phys. Rev. B **88**, 064505 (2013).

[34] O. B. Korneta, Tongfei Qi, S. Chikara, S. Parkin, L. E. De Long, P. Schlottmann, and G. Cao, Phys. Rev. B **82**, 115117 (2010).

[35] T. Shimura, Y. Inaguma, T. Nakamura, M. Itoh, and Y. Morii, Phys. Rev. B **52**, 9143 (1995).

[36] C. Dhital, T. Hogan, W. Zhou, X. Chen, Z. Ren, M. Pokharel, Y. Okada, M. Heine, W. Tian, Z. Yamani, C. Opeil, J. S. Helton, J. W. Lynn, Z. Wang, V. Madhavan, and S. D. Wilson, arXiv:1311.0783.